

ROMUALD KACZYŃSKI

**APPLICATION of FILTERING TECHNIQUES in SPATIAL  
and FREQUENCY DOMAINS FOR IMPROVING ACCURACY of  
SUPERVISED CLASSIFICATION**

*SUMMARY. The results of analysis of the possibility of distinguishing the U.S.A. National Bureau of Standards colour test fields on the basis of pattern recognition using System 600 International Imaging Systems (I<sup>2</sup>S) software and multispectral data are presented. The multispectral four bands data were preprocessed before classification in both spectral and frequency domains using Fast Fourier Transform (FFT technique). Colour fields after maximum likelihood classification were recognized with overall accuracy of 98 per cent for FFT preprocessed image and 99 per cent for image smoothed by Median filter.*

### **1. Introduction**

The analysis of the possibility of distinguishing the NBS 32 colour test fields on the basis of pattern recognition using ERDAS software has been published [2] and presented on 17th ISPRS Congress in Washington D.C. in 1992.

The same digital data in four bands have been used as 'raw' data for digital image processing using powerful I<sup>2</sup>S System 600 software. Raw data have been preprocessed before supervised classification both in spatial and frequency domains. These two preprocessed imageries were used for maximum likelihood classification on I<sup>2</sup>S System 600.

### **2. Reconstruction of the image from its samples**

The raw digital multispectral image represents measurement of photographic density recorded by MB-470 NAC camera on KODAK IR-2424 film as function of colour NBS test  $g(x,y)$ .

Let  $f(x,y)$  denote a continuous photographic ideal image representing object - test  $g(x,y)$ . This image has been scanned using sampling system Scanmaster Howtek [2]. Spatial samples of an image could be obtained as discrete image  $f(k,l)$  in spatial domain  $(k,l)$  by operation

$$f(k,l) = f(x,y) \cdot s(k,l)$$

where  $s(k,l)$  is spatial sampling function composed of an array of Dirac delta function ( $\delta$ ) arranged in a grid of spacing  $x, y$  in  $k$  (columns) and  $l$  (lines) directions [1].

The image  $f(k,l)$  has been taken from the continuous image recorded as  $f(x,y)$  only at the sample points  $(k \Delta x, l \Delta y)$  by sampling function  $s(k,l)$

$$s(k,l) = \sum_{k=-\infty}^{\infty} \sum_{l=-\infty}^{\infty} (x - k\Delta x, y - l\Delta y)$$

The sampling period must be equal to, or smaller than half of the period of the finest detail within the scanned image (at least twice its highest frequency component). It means that photoimage has to be sampled at its Nyquist rate [3]. From sampling theory [3]  $\Delta x = \Delta y < 1/2$  band width. Band width for MB-470 NAC filters are equal about 120 nm [1]. 200 dpi is equivalent to  $x = y = 0.125$  mm. The chosen aperture 200 dpi has satisfied the Nyquist rate.

Exact reconstruction of the image  $f(x,y)$  can be obtained by applying filtering techniques to the sampled discrete image  $f(k,l)$ . Discrete image is represented in vector form by mean value, correlation and covariance-variance matrices. As the colour fields are uniform which means that should contain only low frequency signal of the test fields with small variance values in all bands. Theoretically, all 32 colour test fields as well as background should have constant brightness (DN) values in the  $f(x,y)$  and  $f(k,l)$  images. But the photoimage  $f(x,y)$  has been created by the convolution between the scene (test) radiance  $g(x,y)$  and Optical Point Spread Function of the MB-470 NAC camera which distorted the photographic image of the original object test. Also additional noise (as high frequency signal) has been added to the  $f(k,l)$  image during the scanning process using the colour light beams (R,G,B) of the Scanmaster Howtek. As the result colour test fields have not constant DN values.

The statistics of the scanned image  $f(k,l)$  for all 32 colour test fields are given in [2]. One can see that standard deviations (SD) vary from 0.9 to 17 (variances vary from 0.81 to 290). Only field #267 has small value of SD in all four bands (Black test field).

Applying low-pass filter to sampled image  $f(k,l)$  in spatial domain or to Fourier transformed image  $\mathcal{F}(u,v)$  in frequency domain could improve the image and make it more uniform.

## 2.1. Filtering in frequency domain

If the grey level at position  $(k,l)$  in the region is  $f(k,l)$ , then the discrete two-dimensional Fourier transform of an discrete image  $f(k,l)$  of  $N \times N$  size is obtained by

$$\mathcal{F}(u,v) = \frac{1}{N} \sum_{k=0}^{N-1} \sum_{l=0}^{N-1} f(k,l) \exp\left[\frac{-2\pi i}{N}(uk + vl)\right] \quad \text{for } 0 \leq u, v \leq N-1$$

where  $i = \sqrt{-1}$  and  $u, v$  spatial frequency.

Fast Fourier Transform (FFT) algorithm of I<sup>2</sup>S software value which has been used, requires, that  $N = 2^n$  for  $n=0,1,2,\dots,10$ . Value  $n=8$  has been chosen for the image  $f(k,l)$  where  $k=l=256$  columns by 256 samples (pixels). FFT image contains  $2N^2$  components (the real and imaginary, or phase and magnitude components of each coefficients). As  $\mathcal{F}(u,v)$  exhibits a property of conjugate symmetry [3] almost half of the transform domain components are redundant. Basic functions of FFT are complex exponential that may be decomposed into sine and cosine components (there are also redundancies between these components as well). The spectral component at the origin ( $u=v=0$ ) of FFT is equal to  $N$  times spectral average of the image plane

$$\mathcal{F}(0,0) = \frac{1}{N} \sum_{k=0}^{N-1} \sum_{l=0}^{N-1} f(k,l)$$

This is the zero frequency or DC point (the lowest frequency point) and is displayed as bright area at the centre of RGB display device. Power Spectrum Function (PSF) known also as Spectral Density Function is equal to square root of absolute value of  $\mathcal{F}(u, v)$ :

$$|\mathcal{F}(u,v)|^2 = \mathcal{F}(u,v) * \mathcal{F}^*(u,v)$$

where  $\mathcal{F}^*(u,v)$  is the complex conjugate of  $\mathcal{F}(u,v)$  and could be calculated by I<sup>2</sup>S command CPU'FFT'CONJUGATE  $\mathcal{F}(u,v)$ . PSF could be displayed after scaling as top view (in  $u,v$  coordinates system), or as side view after performing profile on PSF top view display image.

Two functions  $f(k,l)$  and  $\mathcal{F}(u,v)$  are Fourier transform pairs. Every  $f(k,l)$  has unique transform  $\mathcal{F}(u,v)$  and every  $\mathcal{F}(u,v)$  has unique inverse  $f(k,l)$ . CPU'FFT'POWER\_SPECTRUM produce a PSF image. The magnitude of the Fourier coefficients in logarithmic domain could be displayed for analyzing the frequency power distribution of the image as well as for noise and blur assessment.

Top view of the PSF of 'raw' NAC\_FFT\_ band#3 image (size 256x256) is shown on Fig.1. Zero frequency or DC point is at the centre ( $u=v=128$ ) as white area. The conjugate symmetry is easily seen. As the colour test fields are arranged in rectangle 4 by 8 in  $x$  and  $y$  directions, the spread of values (white and black) in PSF are biased in both  $u$  and  $v$  directions with constant interval equal 17.

High frequency (HF) or Nyquist frequency is at the edge of the PSF image in  $u$  direction (horizontal line).

Side view of PSF of 'raw' image NAC\_FFT band #3 (size 256x256) is shown on Fig.2. One can see that the amplitude of different frequencies vary in the range from 100 to 256 (PSF has been compressed to 8-bit data for displaying purpose on RGB device).

Different filters in frequency domain could be applied to the transformed image  $\mathcal{F}(u,v)$ . Band #3 of  $f(k,l)$  image has been used to test filters in frequency

domain using CPU'FFT software of I<sup>2</sup>S System 600. Two images each size 16 x 16 (n=4) of colour fields #39 and #171 were extracted from band#3. FFT has been run for both images with Hamming window to avoid aliasing effects. Gauss filter with DC gain>> HF gain were used to perform low-pass filtering of  $\mathcal{F}(u,v)$ , images (i=1,2). Statistics of raw test fields taken from [1] and smoothed one in frequency domain by Gauss low-pass filter are shown in Table 1. It is seen from table 1 that both images (39 FFT\_Gauss and 171 FFT\_Gauss) after preprocessing in frequency domain have smaller Max-Min values and SD then raw images.

Profiles in the spatial domain of test field #171 raw image (left) and the image created by applying FFT with Gauss low-pass filter (right profile) are shown on Fig.3. It is seen that high spinkle noise has been removed by Gauss filter but additional low DN small noise has been implemented.

Low pass Gauss filter has been implemented to the whole 256x256 band #3 image. PSF top view of image filtered by Gauss function is shown on Fig.4. Side view of this PSF at  $\theta=90^\circ$  is shown on Fig.5. Comparing Fig.2 and Fig.5 one can see that filtered image has less dispersed graph then raw one. Unfortunately still noise has been observed on some of the test fields. FFT'EXPONENTIAL\_FILTER in frequency domain has been applied independently to all 256x256 four bands of raw image transformed to frequency domain by FFT. Profile in spatial domain of test field #264 raw image (left) and filtered image (right) band #1 by exponential filter in frequency domain is shown on Fig.6. From Fig.6 one can see that the right profile is smoothed comparing to the profile on the raw image.

Raw enlarged image size 16 x 16 (one colour test field #171 in one band) as left one and the same test field after FFT processing (as right photo) is shown on Fig.7. Profiles (lines 1 & 2 on Fig.7) of these two images are shown on Fig.8 (raw image) and FFT image on Fig.9. Image after FFT has DN values almost constant (see Fig.9).

After processing of  $\mathcal{F}(u,v)$  image in frequency domain inverse transform was employed to obtain spatial domain 8-bit image. This operation for discrete image is done by applying formula

$$f(k,l) = \frac{1}{N} \sum_{k=0}^{N-1} \sum_{v=0}^{N-1} \mathcal{F}(u,v) \exp\left[\frac{2\pi i}{N}(uk + vl)\right] \quad \text{for } 0 \leq k, l \leq N-1$$

## 2.2. Filtering in spatial domain

Second filtered image has been created by using smoothing filter in spatial domain. The convolution operation in discrete case is given by

$$\begin{aligned} y(k,l) &= h(k,l) * f(k,l) \\ y(k,l) &= \sum_{k'=l'=-\infty}^{\infty} h(k-k', l-l') f(k', l') \end{aligned}$$

MEDIAN\_FILTER, which performs two-dimensional Tukey median filter operations was employed for the raw image. Plus shaped kernel  $w \times w = 3 \times 3$  size has been used for smoothing raw image and high frequency noise removal. Weights of the kernel in the window ( $3 \times 3$ ) = 0,1,0,1,1,1,0,1,0.

For discrete image of size  $N \times N$  ( $265 \times 256$ ) window  $w \times w$  is moving through the array  $f(k,l)$  image and produce new  $f'(k,l)$  image

$$f'(k,l) = \sum_{m=i-w/2}^{w/2} \sum_{n=j-w/2}^{j+w/2} f(k,l) \text{PSF}(i-k,j-l)$$

The first and last lines as well as rows are distorted by this operation.

### 3. Classification of preprocessed images on I<sup>2</sup>S System 600

Two preprocessed images were created from raw digital data, one using FFT filtering technique in frequency domain as NAC\_FFT and one after filtering in spatial domain by MEDIAN\_FILTER as NAC\_MED. Reducing the scene noise effect and smoothing the colour test fields prior to per-pixel classification is highly recommended by many authors [1], [3].

The processing flow of supervised classification procedure on I<sup>2</sup>S System 600 Model 75 is shown on Fig. 10.

Statistical data of the signatures of the image NAC\_FFT after filtering in frequency domain are shown in Table 2. Statistical data of the signatures of the image NAC\_MED are shown in Table 3. One can see that all test fields in both preprocessed images have been smoothed comparing to the raw data (see Table 1 published in [2]). Comparison for three test fields in three images has been constructed (see Table 4) to show the advantage of properly selected filters to be used with the raw image before classification.

Each colour test field consist of  $16 \times 16 = 256$  pixels in one band. More than 50 pixels have been taken as the training samples in each class (colour test field). It is known that statistical separability between classes is related to the area under the probability functions in the region of overlap. Increasing the variance ( $SD^2$ ) of a class increases the probability error. As the all colour test fields (classes) have equal a priori probabilities, the decision boundary were located at the centre of the probability density function. The overlap area decreases as the separation of the mean values of two classes increases. Statistical separability known as divergence of two classes (i.e. separability of their probability density functions) were calculated using mean values and inverse covariance matrices in the four-dimensional space. CPU'CLASS'DIVERGENCE calculates the separability of two classes with given covariance matrices and mean vectors. Calculation is done according to the formula

$$D_{ij} = \text{tr}[(C_i - C_j)(C_j^{-1} - C_i^{-1})] + \text{tr}\{(C_i^{-1} - C_j^{-1})(M_i - M_j)(M_i - M_j)^T\}$$

---

where  $D_{ij}$  - divergence for classes  $i, j$   
 $C_i, C_j$  - the NB by NB covariance matrices of  $i$ -th and  $j$ -th classes  
 $M_i, M_j$  - the NB mean vector of  $i$ -th and  $j$ -th classes for  $i=1$  to NC and  
 $j=1$  to NC,  $i \neq j$   
 $\text{tr}$  - trace of the matrix  
 $T$  - transpose of the matrix

In this case  $NB=4$ ,  $NC=32$  and .PREP file were used as input to this software. The equation is used to calculate divergence for each class pair. Matrix  $NC \times NC$  of pairwise divergences for every combination of NB bands taken B at time (for B from 2 to NB) will be stored/printed. Total  $2^{NB}$  combination of subset of the bands is possible to be evaluated.

Due to so much of the data which produces this program, only average divergence and divergence for two classes for given any pair of feature subset have been calculated. Average divergences and transformed average divergences for different band combinations of NAC\_MED.PREP file are shown in Table 5, and for NAC\_FFT.PREP in table 6. Divergence for two classes for different band combinations are given in Table 7.

One can see from Table 5 and Table 7 that all bands should be taken for classification, specially if classes #183 and #266 have to be recognized. The mean values of colour test field #183 and #267 are very close to each other (see Table 3) as well as colour test field #183 and #266. Please note that these three classes (namely 183,266,267) were merged before classification done by ERDAS software [2].

Maximum likelihood classifier CPU'MLCLASSIFY was employed with equal a'priori probabilities values for each class to classify two preprocessed images NAC\_MED and NAC\_FFT.

#### 4. Evaluation of the classified 'maps'

All image consist of 256 lines by 256 samples= 65,536 pixels

All colour test fields consists of (16 lines by 16 samples)x32 fields= 8192 pixels.

Background consist of  $65,536-8192=57,344$  pixels

These data were used for accuracy assessment of the final maps. The statistics of classified images are shown in Table 8.

In both outputs a certain number of mixed pixels in the similar colour test fields have been observed as shown below:

NAC_FFT image:	118 with 117 (both Yellow-Green)
	168 with 181 (both Blue)
	266 with 267 & 182

183 with 266 & 267 (almost Black)  
38 with 39 (both Orange)  
37 with 35 (both Orange)

NAC\_MED image:      38 with 39  
                        37 with 35  
                        85 with 86 (both Yellow)  
                        139 with 118 (both Yellow-Green)  
                        168 with 181 (both Blue)  
                        183 with 266 & 267 (Black)

After correction and merging classes representing black fields (#183,266,267) final overall accuracy for both images are shown bellow.

	NAC_FFT	NAC_MED
Overall accuracy before correction:	96%	98.2
Overall accuracy after small correction:	98.2%	99%

## 5. Conclusion

The achieved results show that both methods used for filtering raw data in spatial or frequency domains are equivalent and they are strongly recommended to be used before classification. The overall accuracies achieved here by using I<sup>2</sup>S System 600 Software are better then accuracy achieved by using ERDAS software [2]. FFT software is a powerful tool which has not yet been used in OPOLiS- IGiK by analyst of multispectral digital data.

For small kernel size MEDIAN filter is recommended to be used in spatial domain for noise removal and smoothing an image before classification to be performed.

For bigger kernel size FFT is recommended to be used. The disadvantage is that FFT in I<sup>2</sup>S system 600 requires an image of size an integral power of two.

The minimum spectral Euclidian distance in two bands between two classes for I<sup>2</sup>S System 600 software were found to be more then 10.8, so colour test field would be classified with 99 percent accuracy.

The elaborated and tested procedures on colour test were employed to elaborate aerial multispectral photographs of test area KULIN taken by multispectral camera MB-490 NAC. The results will be published separately.

---

### Bibliography

- [1] Anil K. Jain.: *Fundamentals of Digital Image Processing*. Prentice Hall Information and System Sciences Series. New Jersey, USA 1989.
- [2] Kaczyński R.: *Analysis of the possibility of distinguishing colour test taken by Multispectral camera and using ERDAS system*. 1992 T. 39 z. 1(87) s. 137-148
- [3] Prat W.K. *Digital Image Processing*. New York: John Wiley and Sons 1978.
- [4] *System 600 Digital Processing System. Command Reference*, Vol.1, Vol.2. International Imaging Systems, California 1989.

*Recenzował: doc. dr inż. Adam Linsenbarth  
Przyjęto do opublikowania w dniu 27 lutego 1993 r.*

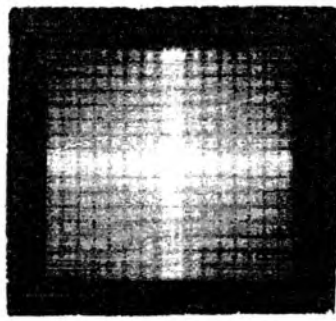


Fig. 1. PSF top view of raw image  
NAC\_FFT band #3

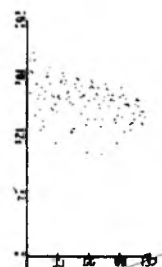


Fig. 2. PSF side view, profile in  
frequency domain of NAC\_FFT raw  
image band #3.  $\theta=90^\circ$



Fig. 3. Profile in spatial domain of test file #171 raw image (left) and image after FFT with Gauss low-pass filter (right)

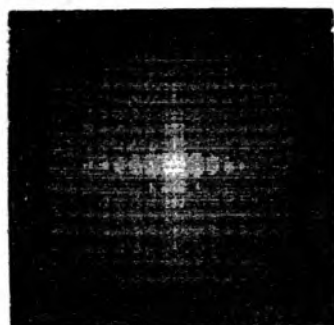


Fig. 4. PSF top view of NAC\_FFT low-pass Gauss filtered image in frequency domain

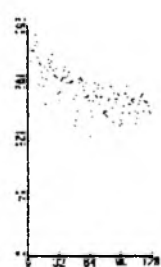


Fig. 5. PSF side view, profile in frequency domain  $\theta = 90$  of NAC\_FFT low-pass Gauss filter



Fig. 6. Profile in spatial domain of test field #171 raw image (left) and image after FFT with Gauss low-pass filter (right profile).

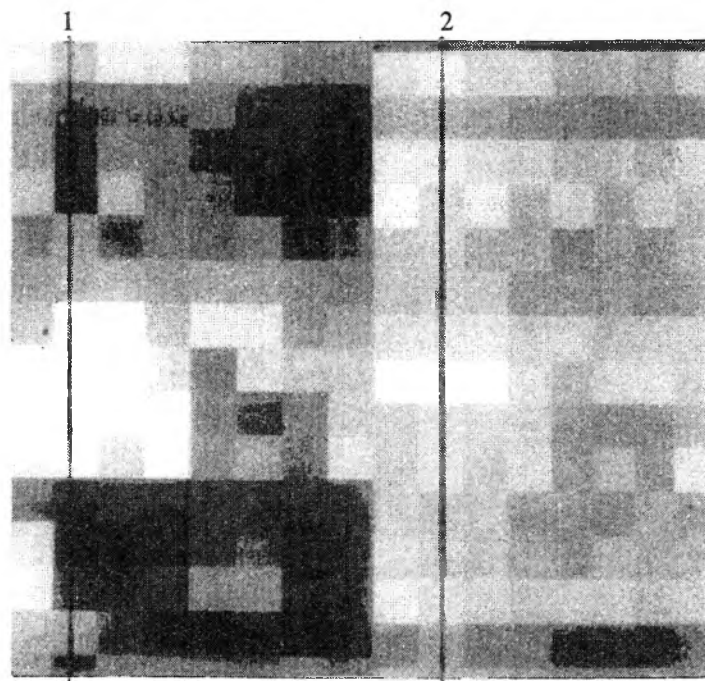


Fig. 7. Enlarged 16 x 16 pixels test field #171. Left (1) is raw image with noise, right (2) is preprocessed image by FFT operations.

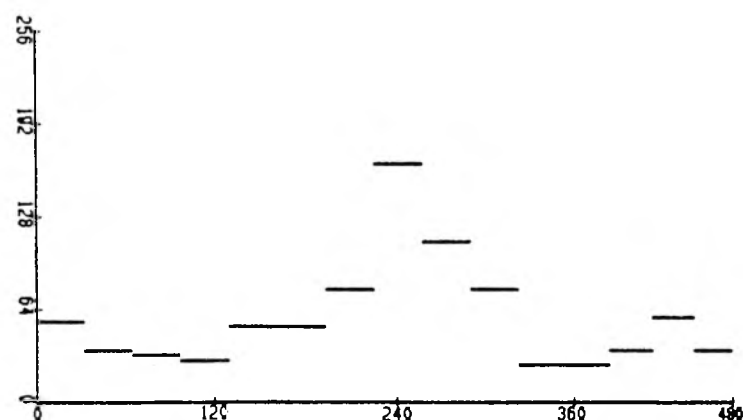


Fig. 8. Profile of raw noisy image (line 1 on Fig.7)

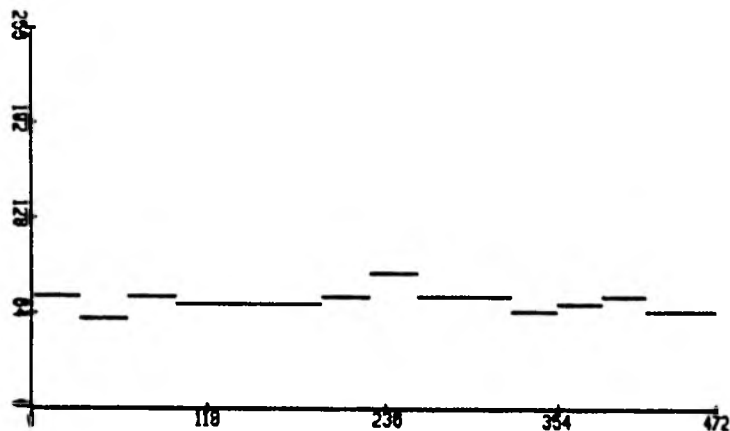
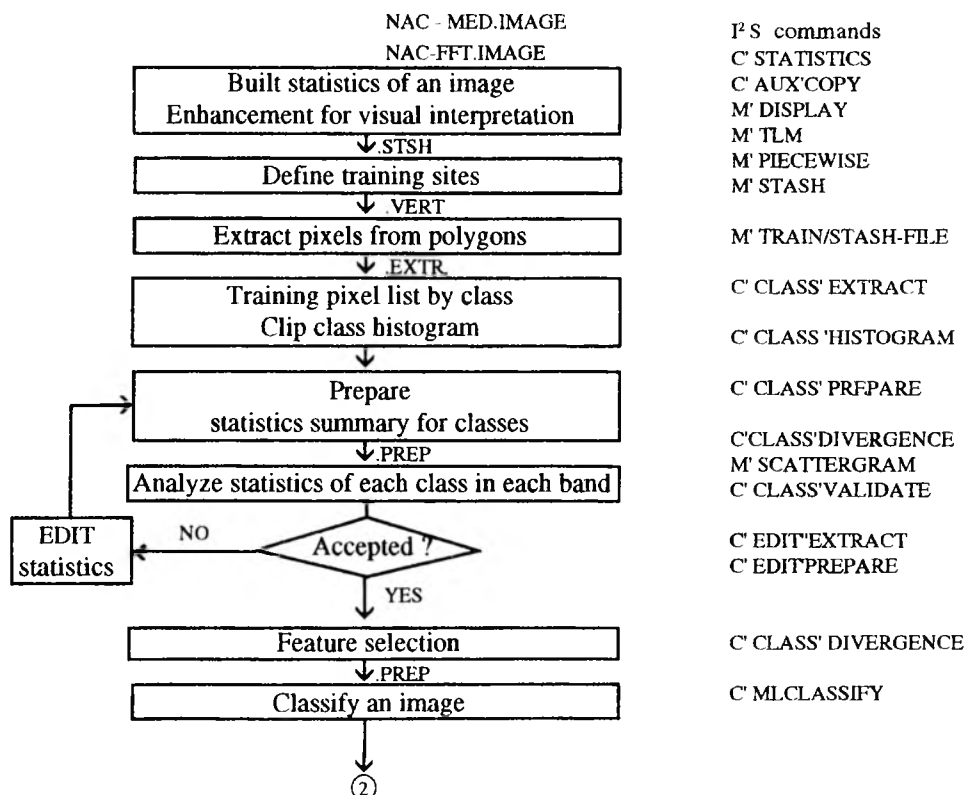


Fig. 9. Profile of FFT preprocessed image (line 2 on Fig. 7)



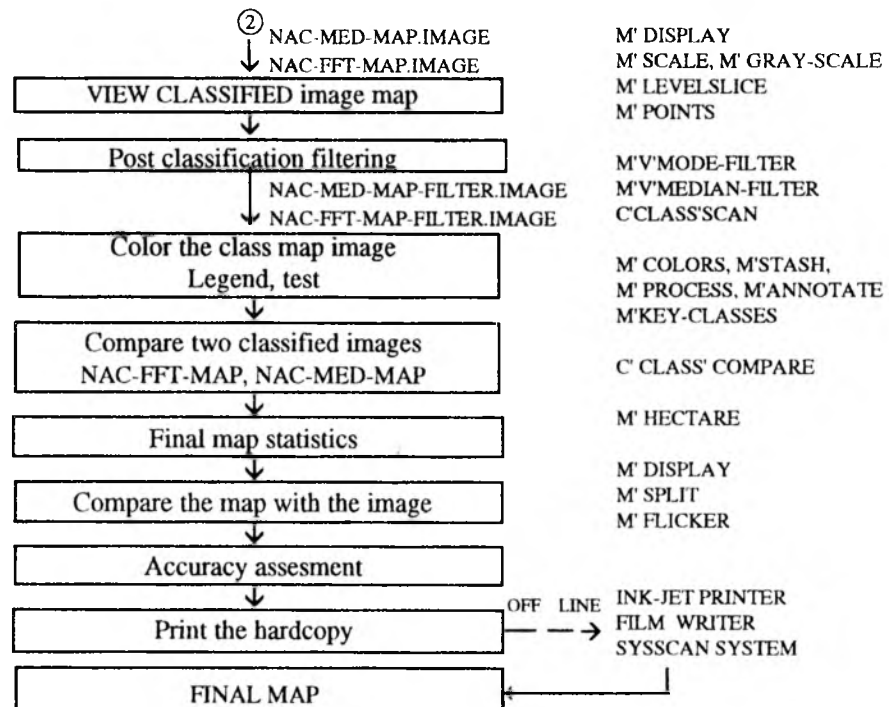


Fig. 10. Flow chart of supervised classification procedures on System 600 Model 75 IIS and software employed to preprocessed NAC-FFT and NAC-MED test images

Statistics of raw and processed by FFT with law-pass

Table 1

Field #	MIN	MAX	MAX-MIN	MEAN	SD	Variancja $SD^2$	Remarks
39 Raw	53	78	25	64	4.6	21.2	Gaussian noise image
39 FFT-GAUSS	13	27	14	19	2.8	7.8	Noiseless image
171 Raw	64	107	43	73	6.5	42.2	Spickle noise image
171 FFT-Gauss	34	64	30	50	5.5	30.2	Noiseless image

Table 2, Page 1  
Statistical data of the signatures NAC\_FFT after Fourier Transform with exponential - filter

Field	Band = 1						Band = 2						Band = 3						Band = 4					
	#	MIN	MAX	MEAN	SD	MIN	MAX	MEAN	SD	MIN	MAX	MEAN	SD	MIN	MAX	MEAN	SD	MIN	MAX	MEAN	SD			
39	9	17	12	1.7	5	8	6.8	0.8	76	93	83.5	4.0	14	18	15.9	1.0								
37	8	13	10	1.2	5	8	6.4	0.6	130	152	140.0	4.6	30	38	33.8	2.0								
35	5	11	8	1.3	5	7	5.9	0.5	147	174	164.3	4.8	43	61	51.6	3.7								
38	5	9	7	1.0	4	6	5	0.7	58	74	66.2	3.6	13	20	15.8	1.6								
70	37	47	42.7	2.3	25	32	29	1.6	212	228	219	3.7	69	84	74	2.7								
67	9	17	12	1.5	15	24	20	2.2	204	235	222.8	7.6	61	88	72	6.5								
66	4	13	6.7	1.3	9	12	10.4	0.8	213	234	223	5.2	77	93	85.4	3.4								
68	4	9	6.9	1.1	9	19	11.1	2.2	186	212	198	5.7	62	74	68.6	2.8								
86	35	60	46.6	5.1	33	44	38.3	2.6	208	235	221.6	5.7	68	92	81.4	5.7								
83	19	27	22	1.7	26	30	27.4	1.0	209	230	220	4.6	67	84	77.9	3.4								
82	4	9	6.4	1.1	13	17	15.5	0.9	202	227	215.4	5.9	78	94	85.1	3.7								
85	2	9	5.9	1.0	5	9	6.8	0.6	71	99	81.3	4.4	22	34	25.8	2.2								
143	89	111	100.6	4.9	36	46	40.0	2.4	68	92	79.4	5.9	34	52	41.9	3.6								
144	37	46	41.2	2.1	16	21	17.7	1.1	36	53	41.4	3.1	13	23	17.7	2.3								
140	23	37	31	3.0	16	22	18.8	1.6	30	43	36.9	3.0	17	26	22.1	2.1								
139	3	11	7.2	1.2	6	9	7.0	0.6	23	32	26.8	1.8	7	12	10.0	1.2								

Statistical data of the signatures NAC\_FFT after Fourier Transform with exponential - filter

Table 2, Page 2

Field	Band = 1						Band = 2						Band = 3						Band = 4					
	#	MIN	MAX	MEAN	SD	MIN	MAX	MEAN	SD	MIN	MAX	MEAN	SD	MIN	MAX	MEAN	SD	MIN	MAX	MEAN	SD			
119	52	65	59	2.9	35	43	38.5	2.0	138	166	151.9	7.0	53	69	60.2	3.3								
116	12	22	16	2.0	25	30	27.5	1.2	109	140	125.6	5.7	54	69	61.5	2.9								
117	4	9	6.6	1.1	7	10	8.4	0.6	31	42	36.8	2.7	12	19	15.4	1.8								
118	3	9	5.8	1.0	4	6	5.2	0.4	23	29	25.9	1.5	6	11	7.7	1.1								
171	139	153	145.3	2.7	49	62	55	3.0	85	135	96.7	8.1	53	82	60.1	5.0								
172	94	112	100.9	4.5	18	27	22	1.9	29	44	38.6	3.1	17	27	21.3	2.4								
168	87	105	97	4.0	17	21	19	1.1	26	36	31.3	2.0	24	34	30.3	2.2								
169	36	50	41.3	2.6	8	11	9.4	0.6	20	30	25.7	1.8	10	15	12.3	1.0								
184	143	153	147.6	2.3	50	58	53.5	1.9	111	137	123.3	6.3	61	72	64.9	2.2								
181	112	136	128	5.9	13	23	18.4	2.2	35	57	40.6	3.3	35	49	43.2	3.3								
182	33	64	45.7	6.6	5	7	6.0	0.5	19	29	24.2	2.0	7	15	10.5	1.7								
183	4	13	7.2	1.5	3	6	4.2	0.6	19	26	22.7	1.5	3	7	4.9	0.9								
264	113	133	124.7	2.9	22	29	25.9	1.4	86	112	94.3	4.5	29	44	34.1	2.4								
265	32	44	36.9	2.2	6	9	7.4	0.7	30	41	34.7	2.3	6	11	8.6	1.4								
266	6	14	9.3	1.3	3	6	4.2	0.6	21	28	24.8	1.8	3	7	5.2	1.0								
267	0	9	3.9	2.8	0	5	2.7	1.9	11	30	20.9	4.9	0	8	3.3	2.4								

Statistical data of the signatures of NAC\_MED image (filtered by MEDIAN in spatial domain)

Table 3, Page 1

Field #	Band = 1				Band = 2				Band = 3				Band = 4			
	MIN	MAX	MEAN	SD	MIN	MAX	MEAN	SD	MIN	MAX	MEAN	SD	MIN	MAX	MEAN	SD
39	15	19	17.5	1.1	10	12	11.3	0.7	59	64	61.4	1.6	25	28	26.6	0.9
37	14	16	14.9	0.6	10	11	10.4	0.5	109	117	112.9	2.5	53	59	56.3	1.5
35	10	14	11.6	1.1	9	10	9.7	0.4	132	140	136.9	1.8	84	96	88.1	3.1
38	9	11	9.7	0.7	7	10	8.4	0.9	43	50	46.4	1.9	23	30	25.8	1.5
70	58	65	61	2.1	46	51	47.7	1.7	181	189	184.7	2.2	119	130	124.2	2.4
67	15	18	16.6	0.7	27	37	32.4	2.9	178	196	187.7	5.1	107	130	117.1	6.3
66	7	11	9.3	0.8	16	18	17.2	0.8	184	195	189.4	3.0	134	149	142.5	3.4
68	9	11	9.9	0.5	15	22	17.4	1.7	159	172	165.0	3.5	108	119	114.0	2.7
86	59	78	67.1	5.3	57	68	63.1	2.5	182	194	188.4	3.1	123	146	135.4	5.3
83	30	33	31.3	1.0	44	50	46.9	1.7	185	191	188.0	1.4	127	138	132.4	2.9
82	8	10	9.1	0.8	24	28	25.7	0.9	178	189	182.9	3.0	133	150	143.3	4.3
85	7	9	8.2	0.5	10	13	11.5	0.8	56	64	59.6	2.2	40	44	42.2	1.2
143	138	151	144.0	3.9	61	70	66.4	2.4	51	65	58.3	3.6	63	78	70.3	3.4
144	55	63	58.6	2.2	27	33	29.6	1.4	22	26	24.1	1.1	25	35	29.1	2.2
140	39	49	45.4	2.4	28	37	32.9	2.5	18	23	21.1	1.4	34	42	37.8	2.2
139	9	11	10.2	0.5	10	13	11.8	0.7	10	12	11.2	0.7	14	19	16.7	1.0

Statistical data of the signatures of NAC\_MED (filtered by MEDIAN in spatial domain)

Table 3, Page 2

Field	Band = 1				Band = 2				Band = 3				Band = 4			
	#	MIN	MAX	MEAN	SD	MIN	MAX	MEAN	SD	MIN	MAX	MEAN	SD	MIN	MAX	MEAN
119	79	89	83.6	2.3	.59	68	62.6	2.2	.116	129	122.7	2.8	.92	105	97.7	3.1
116	20	25	22.0	1.4	.43	48	45.7	1.2	.93	107	100.0	3.2	.96	107	101.7	2.5
117	9	11	10.0	0.6	.13	15	13.7	0.6	.18	22	20.0	1.0	.23	28	25.6	1.2
118	8	9	8.2	0.4	.8	9	8.6	0.5	.9	11	10	0.2	.11	14	12.6	0.8
171	205	210	207.5	1.0	.88	101	92.3	3.3	.67	81	72.8	3.7	.92	109	99.1	3.5
172	138	151	143.3	3.8	.33	41	36.3	2.6	.19	24	21.6	1.4	.32	40	34.7	2.0
168	130	145	138.7	3.5	.30	34	32.0	1.2	.13	16	14.8	0.9	.47	53	50.4	1.7
169	55	63	58.7	2.2	.14	17	15.7	0.8	.9	11	10.3	0.6	.19	22	20.6	0.7
184	207	214	210.3	1.7	.83	94	88.4	2.5	.92	102	96.6	2.6	.104	110	106.9	1.5
181	168	190	183.7	5.4	.24	35	30.2	3.0	.21	25	23.1	0.8	.66	79	71.7	3.7
182	54	78	63.9	5.5	.9	11	10.0	0.3	.7	10	8.4	0.7	.15	21	17.4	1.4
183	8	12	10.0	1.1	.6	8	7.3	0.5	.7	8	7.4	0.5	.8	9	8.4	0.5
264	174	181	177.4	1.8	.40	46	42.6	1.7	.68	76	71.1	1.9	.53	61	56.2	1.7
265	50	56	53.0	1.3	.11	14	12.6	0.6	.17	20	18.5	0.9	.13	15	14.1	0.6
266	11	14	13.1	0.8	.6	8	6.9	0.6	.8	10	9.0	0.5	.8	10	8.5	0.6
267	7	8	7.8	0.4	.6	7	6.5	0.5	.8	9	8.3	0.5	.7	9	7.6	0.7

Comparision statistical data of three images

Table 4

Field #	Band = 1		Band = 2		Band = 3		Band = 4	
Image	$\Delta$	SD	$\Delta$	SD	$\Delta$	SD	$\Delta$	SD
# 39 Raw	13	2.3	8	1.5	2.5	4.6	21	2.5
NAC_FFT	8	1.7	3	0.8	1.7	4.0	4	1.0
NAC_MED	4	1.1	2	0.7	0.5	1.6	3	0.9
# 86 Raw	45	10	34	7.5	29	5.7	43	9.9
NAC_FFT	25	5.1	11	2.6	27	5.7	24	5.7
NAC_MED	19	5.3	11	2.5	12	3.1	23	5.3
# 171 Raw	29	4.3	37	6.8	43	6.5	50	6.5
NAC_FFT	14	2.7	13	3.0	30	5.5	29	5.0
NAC_MED	5	1.0	13	3.3	14	3.7	17	3.5

$\Delta$  = MAX DN value - MIN DN value

Average divergences of NAC\_MED.PREP

Table 5

Bands Combinations	D average	Transformed D average	Rank
1, 2, 3, 4	16138	49.99	1st
1, 3, 4	15240	49.94	2nd
1, 2, 3	14328	49.93	3rd
2, 3, 4	10321	49.84	4th
1, 2, 4	8653	49.77	5th

Average transformed divergence of NAC-FFT.PREP

Table 6

Bands Combinations	Average transformed Divergence	Rank
1, 2, 3, 4	49.81	1st
1, 2, 3	49.73	2nd
1, 3, 4	49.69	3rd

Divergence for two-classes for different band combinations  
NAC-MED.PREP

Table 7

Class # Class #	Class name Class name	Bands Combinations			
		1, 2, 3, 4	1, 3, 4	1, 2, 3	2, 3, 4
25 - 29	183 - 267	96.39	95.66	96.16	52.96
25 - 28	183 - 184	100.00	100.00	99.99	99.95
25 - 30	183 - 266	96.40	96.56	95.96	75.53
29 - 30	267 - 266	100.00	99.99	98.95	54.60

Final statistics of classified preprocesed images

Table 8

Class name	Colour name	Number of pixels		Remarks
		NAC_FFT	NAC_MED	
38	d. ro	250	256	Red - Orange colours
35	s. ro	250	253	
37	m. ro	262	261	
39	gy. ro	263	260	
68	s. 0Y	260	261	Orange - Yellow
66	v. 0Y	254	254	
67	brill 0Y	257	262	
70	I0Y	245	250	
85	deep Y	251	241	Yellow
82	Y	256	253	
83	brill Y	256	260	
86	IY	267	261	
139	v.G	257	256	Green
140	brill G	261	257	
144	I.G	260	256	
193	v.I.G	258	256	
118	deep YG	266	256	Yellow - Green
117	s.YG	267	256	
116	brill YG	256	256	
119	L.Y.G	257	256	
169	s.g.B	250	261	Blue
168	brill gB	254	256	
172	L.g.B	257	261	
171	v.L.g.B	249	256	
182	m.Blue	252	252	Blue
181	l.Blue	254	256	
184	v.p Blue	263	256	
265	med Gray	259	254	Gray
264	L.Gray	256	256	
183	d.Blue	248	254	These three have been added
267	Black	249	254	
266	deep Gray	248	254	
	Total pixels	8192	8192	
	Total correct	8042	8109	
	Total incorrect	150	83	
	Overall accuracy	98.2 %	99.0 %	

ROMUALD KACZYŃSKI

ZASTOSOWANIE TECHNIK FILTRACJI PRZESTRZENNEJ  
I CZĘSTOTLIWOŚCIOWEJ W CELU POPRAWIENIA  
DOKŁADNOŚCI KLASYFIKACJI NADZOROWANEJ

Streszczenie

W artykule przedstawiono rezultat badań możliwości rozróżniania testów barwnych z użyciem cyfrowej analizy obrazu zdjęć wielospektralnych, przeprowadzonej na Systemie 600 International Imaging Systems Model 75 (I<sup>2</sup>S).

Rezultat badań możliwości wyróżniania testów barwnych, zarejestrowanych kamerą MB-470 NAC i opracowanych metodą cyfrowej analizy obrazu z wykorzystaniem skanera Howtek i systemu ERDAS, opublikowano w [2] oraz zaprezentowano na XVII kongresie Międzynarodowego Towarzystwa Fotogrametrii i Teledetekcji w Waszyngtonie w 1992 r.

Te same zdjęcia wielospektralne zostały przetworzone cyfrowo z zastosowaniem filtracji przestrzennej i częstotliwościowej (transformacje Fouriera), a następnie opracowane za pomocą cyfrowej analizy obrazu metodą klasyfikacji nadzorowanej na Systemie 600 I<sup>2</sup>S.

Zdjęcia wielospektralne, reprezentujące funkcję ciągłą  $f(x, y)$ , zostały przetworzone na postać cyfrową jako funkcja  $f(k, l)$  skanerem z aperturą 200 dpi (dpi - punktów na cal), co spełnia wymagania tzw. progu Nyquist [3].

Teoretycznie biorąc wszystkie 32 barwne pola testowe zarejestrowane jako  $f(k, l)$  powinny charakteryzować stałe wartości odpowiedzi spektralnej (DN) o małej wartości wariancji. Z uwagi jednak na fakt wykonywania zdjęć kamerą MB-470 NAC, charakteryzującą się optyczną funkcją przenoszenia obrazu, OTF<1, szumami spowodowanymi emulsją filmu Kodak IR 2424, jak również wpływem skanowania skanerem Howtek, warunek ten w praktyce nie jest spełniony.

Dane statystyczne dla 32 barwnych pól testowych zamieszczone w tablicy 1 w [2]. Z tablicy 1 [2] wartość wariancji waha się w przedziale od 0.81 do 290. Zastosowanie filtracji do zdjęcia  $f(k, l)$ , pomoże wyrównać i zniwelować tak duże rozpiętości wartości wariancji dla poszczególnych pól testowych [1].

Transformację Fouriera (FFT- Fast Fourier Transform) zastosowano do zdjęcia cyfrowego  $f(k, l)$ , otrzymując w rezultacie nowe zdjęcie oznaczone jako  $\mathcal{F}(u, v)$ . Point Spread Function (widok z góry) kanału nr 3 (Red) testu barwnego pokazano na rys. 1. Widok profilu z boku obrazu PSF pokazano na rys.2.

Do obrazu  $\mathcal{F}(u, v)$  mogą być zastosowane różne filtry cyfrowe w przestrzeni częstotliwościowej z bogatego zestawu oprogramowania Systemu 600 I<sup>2</sup>S. Testowanie różnych filtrów i ich parametrów przeprowadzono na polach testowych nr 39 i nr 171. Filtr Gaussa, przepuszczający niskie częstotliwości, a zatrzymujący wysokie (jakimi są w tym przypadku szумy), zastosowano w przestrzeni Fouriera do obrazu  $\mathcal{F}(u, v)$ , otrzymując nowy obraz charakteryzujący się wyrównanymi wartościami odpowiedzi spektralnej (DN). Statystyczne dane zdjęcia oryginalnego ("surowego") i przetworzonego dla dwóch pól testowych zamieszczone w tablicy 1.

Profil testu nr 171 (surowy obraz z lewej) i testu po filtracji częstotliwościowej (profil z prawej) pokazano na rys. 3.

Widok z góry PSF obrazu filtrowanego filtrem Gaussa niskich częstotliwości pokazano na rys.4, a widok profilu z boku dla  $\theta = 90$  na rys.5.

Filtr wykładniczy, realizujący podany poniżej wzór

$$H(\mathcal{F}) = \alpha + \beta \exp(\gamma * ECC)$$

zastosowano do obrazu  $\mathcal{F}(u, v)$ , otrzymując nowy obraz. Profil zdjęcia surowego i po przetworzeniu pokazano na rys. 6, a powiększone zdjęcia pola testowego w jednym kanale, zarejestrowanego na przetworniku cyfrowo-analogowym MATRIX 3000 firmy Agfa, pokazano na rys. 7. Profile (linie 1 i 2 na rys. 7) tych dwóch zdjęć pokazano na rys. 8 (zdjęcie surowe) i zdjęcie przetworzone na rys. 9.

W wyniku przetworzeń w przestrzeni fourierowskiej i filtracji częstotliwościowej otrzymano zdjęcie NAC\_FFT.IMAGE.

Drugie zdjęcie NAC\_MED.IMAGE otrzymano w wyniku filtracji przestrzennej, tzw. metodą maski (okna) o wymiarze 3 kolumny x 3 wiersze i współczynnikach:

$$\begin{matrix} 0 & 1 & 0 \\ 1 & 1 & 1 \\ 0 & 1 & 0 \end{matrix}$$

Klasyfikację nadzorowaną przeprowadzono zgodnie z opracowanym przez autora schematem pokazanym na rys. 10.

Dane statystyczne pól treningowych dla zdjęcia NAC\_FFT zamieszczone w tablicy 2, a dla zdjęcia NAC\_MED w tablicy 3.

W tablicy 4 zamieszczone (w celu porównania) dane statystyczne trzech barwnych pól testowych trzech zdjęć (oryginał, zdjęcie po filtracji częstotliwościowej i po filtracji przestrzennej metodą maski).

W tablicy 5 zamieszczone wartości średnie dywergencji dla NAC\_MED, a w tablicy 6 dla NAC\_FFT.

W tablicy 7 zamieszczone wartości dywergencji dla par najtrudniej rozpoznawalnych pól i różnych kombinacji kanałów kamery MB-470 NAC. Proszę zwrócić uwagę, że klasy nr 183, nr 266, nr 267 nie były połączone przed klasyfikacją, tak jak to uczyniono w przypadku opracowania na systemie ERDAS [2].

W wyniku klasyfikacji nadzorowanej na Systemie 600 I<sup>2</sup>S obu przetworzonych zdjęć otrzymano średnią dokładność rozpoznania pól testowych 98 % dla zdjęcia NAC\_FFT i 99 % dla zdjęcia NAC\_MED. Wynika z tego wniosek, że obie filtracje są sobie równoważne, a dokładność rozpoznania po filtracji jest większa aniżeli w przypadku jej ograniczonego użycia (patrz [2]), gdzie otrzymano dokładność rzędu 96 %).

Przeprowadzona analiza wykazała również, że minimalna odległość spektralna (dla dwóch najbardziej informatycznych kanałów: RED i IR) powinna być większa niż 10 jednostek, co potwierdza wnioski zamieszczone w [2], otrzymane dla zdjęć opracowanych na systemie ERDAS.

Powыższe badania wykorzystano do przeprowadzenia klasyfikacji na Systemie I<sup>2</sup>S zdjęć wielospektralnych naturalnego obiektu testowego KULIN, zarejestrowanego wielospektralną kamerą lotniczą MB-490 NAC. Wyniki tych badań będą przedmiotem odrębnej publikacji.

## РОМУАЛЬД КАЧИНЬСКИ

ПРИМЕНЕНИЕ ТЕХНИК ПРОСТРАНСТВЕННОЙ И ЧАСТОТНОЙ  
ФИЛЬТРАЦИИ ДЛЯ ПОВЫШЕНИЯ ТОЧНОСТИ КЛАССИФИКАЦИИ  
"С УЧИТЕЛЕМ"

## Резюме

В статье представлен результат исследований по возможности выделения цветных тестов многоспектральных снимков выполненных камерой MB-470 NAC, преобразованных в цифровой вид и обработанных в системе 600 International Imaging System (I<sup>2</sup>S).

Из статистических данных 32 цветных тестовых полей, замещенных в [2], вытекает, что вариации колеблются в пределах от 0,81 до 290. Применение фильтрации для исходных снимков  $f(k,l)$  поможет уравнивать и нивелировать большие колебания вариации для отдельных полей.

Трансформация Фурье (FFT) была применена для цифрового снимка, в результате был получен новый снимок  $\mathcal{F}(u,v)$ , для которого были применены разные фильтры в фурьеовском пространстве (между прочим, фильтр Гаусса, показательный фильтр). Второй снимок был получен в результате пространственной фильтрации с применением фильтра Медиан. Статистические данные обработанных снимков замещены в таблицах 5 и 6.

Классификация "с учителем" проводилась согласно с разработанной автором схемой, помещенной на рис. 10. В результате классификации была получена средняя точность опознавания тестовых полей: 98 % для изображения преобразованного в фурьеовском пространстве и 99 % для изображения обработанного с помощью пространственной фильтрации.

Отмечено улучшение точности классификации по сравнению со снимками преобразованными в ограниченном диапазоне и обработанными в системе ERDAS [2].

Установлено, что минимальное спектральное расстояние между двумя классами должно быть больше 10 единиц, что подтверждает результат полученный в системе ERDAS, а опубликованный в [2].

Перевод: Róża Tołstikowa